A Novel And Tractable Antenna Selection in Spatial Modulation Systems

Yuanyuan He, *Member, IEEE*, Saman Atapattu, *Member, IEEE*, Jamie S. Evans, *Member, IEEE* and Chintha Tellambura[†], *Fellow, IEEE*

Electrical and Electronic Engineering, The University of Melbourne, Australia

[†] Electrical and Computer Engineering, University of Alberta, Canada

***Abstract*—A novel opportunistic antenna selection aided spatial modulation, called opportunistic spatial modulation (OSM), is proposed, which exhibits an attractive system reliability enhancement with low complexity. Its unique features enable a comprehensive analytical framework, which is challenging to acquire with existing transmit-antenna-selection-aided spatial modulation (TASS-SM) schemes. Closed-form expression of improved union bound of the average symbol error probability (ASEP) of proposed OSM-MISO system is derived. Furthermore, we compare the proposed OSM with a prevalent existing TASS-SM scheme to confirm the feasibility and effectiveness of our scheme. Simulation results are provided to corroborate the analytical results.**

***Index Terms*—Antenna selection, multiple-input single-output, spatial modulation, symbol error probability.**

I. Introduction

Spatial modulation (SM) is recently emerging as a promising research field to overcome some drawbacks of conventional multiple-input multiple-output (MIMO), such as, inter-antenna synchronization, ICI, high complexity and huge energy consumption, by activating only one of multiple available transmit antennas with a single-RF chain for each transmission. However, for each channel use, SM achieves higher spectral efficiency (SE) than that of conventional single-antenna transmission via transmitting a 3D modulation signal by combining the antenna-index modulation as well as the conventional 2D signal modulation (such as QAM/PSK) [1].

SM is an open-loop scheme, as the active transmit antenna is randomly determined by the spatially modulated information bits [2]. However, the system is likely to transmit with errors if the channel of active antenna is in highly faded condition. To circumvent such scenario, some closed-loop SM schemes have been proposed by exploiting CSI at the transmitter (CSIT) to improve system reliability. Transmit antenna subset selection-aided SM (TASS-SM), i.e., implementing SM based on selected antennas subset instead of all the transmit antennas, is an attractive such adaptive strategy to boost the reliability of SM [3]–[16]. A capacity optimized TASS (COAS) scheme was introduced for SM-MIMO system in [3], which does not offer transmit-diversity but increases the coding gain. An antenna correlation based TASS was also developed in [4]. Euclidean distance (ED) optimized based TASS (EDAS) scheme has shown to be able to offer high transmit diversity gains for SM-MIMO system, which maximizes the minimum ED of the received SM constellation (error performance), by performing exhaustive search over all the possible antenna subset [5]. The diversity order of EDAS-SM was quantified by [6]. Nevertheless, the excellent performance of EDAS-SM scheme is gained at the cost of high computational complexity. Subsequently, a number of work has focused on complexity reduction of EDAS-SM schemes, via either cutting the complexity of evaluating ED [3], [7], [8], [13] or reducing the search complexity burden [4], [9]–[12], [14]. While recently, more practical scenarios of EDAS-SM systems were examined in [15] with a realistic error-infested feedback channel and in [16] by considering frequency selective channels. However, most of existing TASS-SM are heuristic schemes, which, unfortunately, lead to performance analysis intractable or extremely difficult. For example, although the COAS-SM is one of the simplest TASS-SM schemes, its explicit error performance analysis is limited and almost unexplored [3].

To the best of our knowledge, analytical modeling/ frameworks for TASS-SM are rarely studied in the literature to date. To fulfill this research gap, in this paper, we propose a novel low-complex TASS-SM scheme, called Opportunistic Spatial Modulation (OSM) , by judiciously combining the opportunistic antenna selection and SM to significantly enhance the system reliability. Its unique features enable us to develop a comprehensive analytical framework of OSM over Rayleigh fading channels. Note that, we focus on MISO systems for simplicity, but it can easily be extended to MIMO systems by conducting a priori single-antenna selection on receiver. The key technical contributions of this paper are: 1). We propose a novel and tractable antenna selection scheme in SM systems called OSM. A complete derivation of explicit expression of error performance of OSM-MISO system, based on accurate 'improved unionbound' method, is presented, which is highly challenging to quantitatively characterize with existing TASS-SM schemes. 2). We also compare the proposed OSM with prevalent low-complex COAS-SM scheme. Our OSM outshines COAS-SM in terms of analytical tractability, reduced CSI feedback bits, low complexity and superior performance as SNR increases, which implies our OSM scheme is a more efficient low-complexity TASS-SM scheme. 3). The proposed OSM analytical framework also opens up a new avenue for possible designing the TASS-SM schemes with all the key merits of tractability, low-complexity and high diversity order.

II. Opportunistic Spatial Modulation (OSM)

We consider an OSM-MISO system as shown in Fig.1, which consists of a MISO wireless link with N_{t} transmit

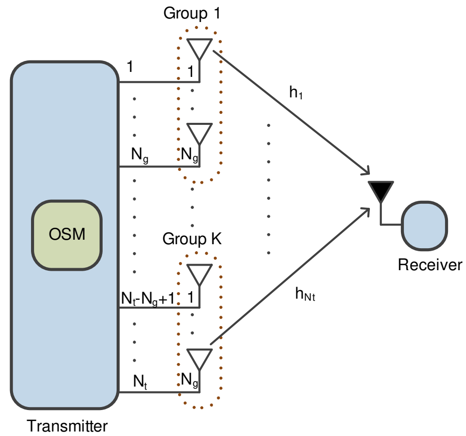

Fig. 1. Illustration of the OSM-MISO system model.

antennas. The cardinality of the APM signal constellation diagram is denoted by M ($M \geq 2$). We assume both $N_{\rm t}$ and M are to be power of two. All the channels involved are assumed to be iid Rayleigh fading. The transmitter-to-receiver channel is denoted by $\mathbf{h} = [h_1, \cdots, h_j, \cdots, h_{N_t}] \in \mathbb{C}^{1\times N_{\rm t}}$, where the entry h_j is the channel coefficient between the jth transmit antenna to the receiver, and $h_j \sim \mathcal{CN}(0, 1)$.

The idea of OSM scheme is to opportunistically select the transmit antennas subset as the new spatial-constellation diagram for SM, and is thus called as *opportunistic SM (OSM)* scheme. More specifically, OSM scheme follows two steps: i) the antenna selection, and ii) the conventional SM implementation. Step I: At the transmitter, $N_{\rm t}$ transmit antennas are equally split into K groups (K is also assumed to be a power of two). Let $N_{\rm g} \triangleq \frac{N_{\rm t}}{K}$. For each Group k, $k \in [1, K]$, the antenna with the largest channel gain is selected for the later SM transmission, where the selected antenna index and the corresponding channel are represented by $N_{(k)}$ and $g_{(k)}$, respectively, and given as $N_{(k)} = \arg\max_{i\in[(k-1)N_g+1, kN_g]} |h_i|$ and $|g_{(k)}| = \max_{i\in[(k-1)N_g+1, kN_g]} |h_i|$. Step II: The conventional SM technique is implemented based on the selected K antennas $\{N_{(1)}, \cdots, N_{(K)}\}$ and $M-$ary APM symbols.

Thus, in the OSM scheme, the information bits are conveyed via both the spatial constellation represented by K different antenna index set $\{N_{(1)}, \cdots, N_{(K)}\}$, and the M-ary APM signal constellation comprised of symbols set $\{s_1, \ldots, s_M\}$ ($\mathbb{E}[|s_m|^2] = 1$), given as $B = \log_2(K) + \log_2(M)$ bpcu. The first $\log_2(K)$ bits are used to choose an unique antenna index from $\{N_{(1)}, \cdots, N_{(K)}\}$, and the other $\log_2(M)$ bits are used to map an APM symbol from $\{s_1, \ldots, s_M\}$. Then at each transmission, only one of the K selected antennas is activated for transmitting the mapped APM symbol while all the other antennas remain in silent. **Example:** The OSM mapping principle is shown in Fig. 2 for a transmitter with $N_{\rm t} = 4$, $K = 2$ and the BPSK modulation. We then have $B = \log_2(2) + \log_2(2) = 2\,\text{bpcu}$, where one bit is encoded in the antenna group indexes(the bit "0" for Group 1 and "1" for Group 2), and the other bit is encoded in the BPSK symbols (the bit "1" for $s_1 = +1$ and"0" for $s_2 = -1$). Given binary input bits "01", it means the first antenna (which is the 'best'

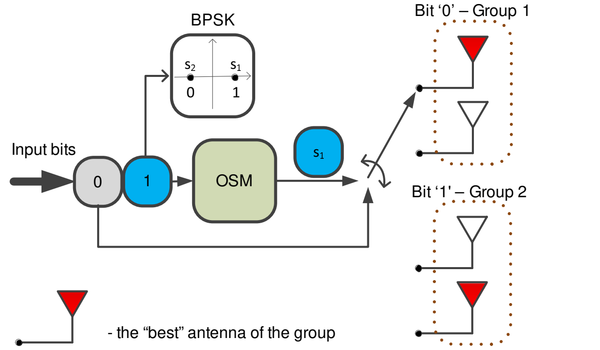

Fig. 2. Illustration of OSM bit-to-symbol mapping rule for $N_{\rm t} = 4, K = 2$, BPSK case.

antenna of Group 1) will be activated to emit the s_1.

It is easy to find that when $K = N_{\rm t}$, the OSM-MISO scheme reduces to the conventional SM-MISO system; when $K = 1$, the OSM-MISO scheme reduces to the conventional MISO with the 'best' single transmit antenna selection scheme (TAS-MISO). For encoding and decoding purposes, the opportunistic antenna selection rules and the OSM mapping rules are assumed to be known by both the transmitter and receiver a priori. However, the transmitter does not required to access full CSI. This can be achieved by assuming that the receiver can correctly estimate the full CSI and sends the indexes $\{N_{(1)}, \cdots, N_{(K)}\}$ to transmitter via a perfect feedback link.

For a given transmission instance, only one transmit antenna is in active. Without loss of generality, the transmission of Group k with symbol s_m is elaborated here. Thus, the transmitted signal can be given as $\mathbf{x}_{k,m} = \mathbf{A}\Upsilon_k s_m$, where $\mathbf{x}_{k,m} \in \mathbb{C}^{N_{\rm t}\times 1}$; $\mathbf{A} \in \mathbb{C}^{N_{\rm t}\times N_{\rm t}}$ is a diagonal matrix denoted as $\mathbf{A} = \text{diag}(a_1, ..., a_{N_t})$, with $a_i = 1$ if the i-th antenna is selected as the 'best' antenna in one of the antenna group, i.e. $i \in \{N_{(1)}, \cdots, N_{(K)}\}$, otherwise $a_i = 0$; $\Upsilon_k \in \mathbb{C}^{N_{\rm t}\times 1}$ indicates that the antenna Group k is chosen by first $\log_2(K)$ information bits, which is given as

$$\Upsilon_k \triangleq \underbrace{[0\ldots0\;1\ldots1\;0\ldots0]^T}_{\text{From } (k-1)N_{\rm g}+1 \text{ to } kN_{\rm g} \text{ entries are "1"}}; \tag{1}$$

and s_m is one of the APM symbols determined by the rest $\log_2(M)$ information bits. Then, the received signal at the receiver of OSM-MISO, denoted as y, can be given as

$$y = \mathbf{hA}\Upsilon_k s_m + n \overset{(a)}{=} \sum_{j=(k-1)N_{\rm g}+1}^{kN_{\rm g}} a_j h_j s_m + n \overset{(b)}{=} g_{(k)} s_m + n$$

where $n \sim \mathcal{CN}(0, \sigma^2)$ is the additive white Gaussian noise; (a) follows as we consider Group k transmission; (b) follows as Group k has only one active antenna $N_{(k)}$ with corresponding channel $g_{(k)}$. OSM-MISO can be treated as conventional SM-MISO with effective channels $\mathbf{g} \in \mathbb{C}^{1\times K} = [g_{(1)}, \cdots, g_{(K)}]$.

Therefore, similar to conventional SM-MISO, the maximum likelihood (ML) detection criterion is adopted at the receiver of our OSM-MISO to jointly decode both the active antenna group index and the transmitted symbol, given as, $(\hat{k}, \hat{m}) = \arg\min_{k\in[1,K], m\in[1,M]} |y - g_{(k)} s_m|^2$. An important performance measure for the ML detector is the symbol error probability (SEP). Define $\mathbb{X}$ as the set of all possible OSM transmit signal vectors, i.e., $\mathbb{X} = \{\mathbf{x}_{k,m} = \mathbf{A}\Upsilon_k s_m | k = 1,\ldots,K;\ m = 1,\ldots,M\}$, with the size $|\mathbb{X}| = KM$. We assume all the elements of $\mathbb{X}$ to be equally likely. It is easy to find that each signal vector has only one non-zero element, and the dissimilar between any two signal vectors $\mathbf{x}_{k,m}$ and $\mathbf{x}_{k',m'}$ is either one element or two elements. The first situation occurs when $\mathbf{x}_{k,m}$ and $\mathbf{x}_{k',m'}$ have same active antenna group index(i.e., $k = k'$); while the second situation happens when they have different antenna activation position (i.e., $k \neq k'$).

Based on above mentioned two situations, the average SEP (ASEP), denoted as P_S, can be calculated as [17]

$$P_S = \frac{1}{K}\sum_k P_{s_{\text{singal}}}(k) + \frac{1}{KM}\sum_k \sum_{k'\neq k}\sum_m \sum_{m'} \mathbb{E}_{\mathbf{h}}\left[\Pr\{\mathbf{x}_{k,m} = \mathbf{x}_{k',m'} | \mathbf{x}_{k,m}\}\right] \tag{2}$$

where $P_{s_{\text{singal}}}(k) = \frac{1}{M}\sum_m \sum_{m'\neq m} \mathbb{E}_{g_{(k)}}\left[\Pr\{s_m = s_{m'} | s_m\}\right]$. We can interpret (2) as follows: (1) The first term $\frac{1}{K}\sum_k P_{s_{\text{singal}}}(k)$ corresponds to the ASEP of OSM-MISO when $k = k'$. It means that only the symbol is wrongly detected, and $P_{s_{\text{singal}}}(k)$ can thus be regarded as the ASEP of a conventional TAS-MISO for a given Group k. (2) The second term is the ASEP of the OSM-MISO when $k \neq k'$, which implies that the antenna group index is detected incorrectly.

The exact analysis of the P_S in (2) is an arduous task due to the intricate 2nd term. However, due to the low implement complexity of OSM-MISO, the low-moderate SNR performance can be easily obtained via Monte Carlo, and the computational difficulty only exists in getting the high-SNR performance. Therefore, here we focus on obtaining a exact upper bound performance, which is highly accurate in high-SNR. For this purpose, it is natural to consider conventional union-bound. But the challenge in (2) is only the 2nd term, we will apply the union-bound to 2nd term only. This is known as "Improved Union-bound" [17], a tighter upper bound for ASEP. Denoting such bound as P_{IU}, it can be formulated as,

$$P_S \leq P_{IU} = \frac{1}{K}\sum_k P_{s_{\text{singal}}}(k) + \frac{1}{KM}\sum_k \sum_{k'\neq k}\sum_m \sum_{m'} \text{APEP}_{(k,m)\to(k',m')} \tag{3}$$

where $\text{APEP}_{(k,m)\to(k',m')}$ is average pairwise error probability (APEP) of $\mathbf{x}_{k,m}$ being erroneously decoded as $\mathbf{x}_{k',m'} \in \mathbb{X}$,

$$\begin{aligned}\text{APEP}_{(k,m)\to(k',m')} &\triangleq \mathbb{E}_{\mathbf{g}}[\Pr(|y - g_{(k)}s_m|^2 \geq |y - g_{(k')}s_{m'}|^2 | \mathbf{g})] \\ &= \mathbb{E}_{\mathbf{g}}\left[Q\left(\sqrt{\frac{|g_{(k)}s_m - g_{(k')}s_{m'}|^2}{2\sigma^2}}\right)\right],\end{aligned} \tag{4}$$

with $Q(\cdot)$ being the Gaussian Q-function.

III. Performance Analysis of OSM-MISO

A. Explicit Error Performance of OSM-MISO

In this section, we derive the closed-form expression for the improved-upper bound of the ASEP given in (3) with PSK signal modulation. We first derive the exact expression for the first term of (3), i.e., $\frac{1}{K}\sum_k P_{s_{\text{singal}}}(k)$. As $P_{s_{\text{singal}}}(k)$ can be considered as the exact ASEP of the conventional TAS-MISO with the selected best channel $g_{(k)}$, according to [18, eq.(30)] [19, eq.(5.66)], $P_{s_{\text{singal}}}(k)$ only depends on the distribution of its channel gain $|g_{(k)}|^2$. Given all the channels are iid Rayleigh fading distributed, according to [20] , the pdf distribution of the selected best channel gain for $k-$th antenna group (denoted as $z_k = |g_{(k)}|^2 = \max_{i\in[(k-1)N_{\text{g}}+1, kN_{\text{g}}]} |h_i|^2$) is given as

$$f(z_k) = N_{\text{g}}\left(1 - e^{-z_k}\right)^{N_{\text{g}}-1} e^{-z_k}, \quad k = 1,\ldots,K, \tag{5}$$

As all $|g_{(1)}|^2,\ldots,|g_{(K)}|^2$ are also iid, we can obtain $P_{s_{\text{singal}}}(1) = \cdots = P_{s_{\text{singal}}}(K) \triangleq P_{s_{\text{singal}}}$, i.e., $\frac{1}{K}\sum_k P_{s_{\text{singal}}}(k) = P_{s_{\text{singal}}}$. Then based on [19] [18] and the distribution (5), the closed-form expression for $P_{s_{\text{singal}}}$ with the $M-$PSK modulation is given in the following Proposition 1.

Proposition 1: With M-PSK modulation, the exact expression of $P_{s_{\text{singal}}} = P_{s_{\text{singal}}}(k), \forall k$ is

$$P_{s_{\text{singal}}} = \frac{M-1}{M} - \sum_{n=0}^{N_{\text{g}}-1}\binom{N_{\text{g}}}{n+1}\frac{(-1)^n}{\pi}\sqrt{\frac{\sin^2\left(\frac{\pi}{M}\right)}{\sigma^2(1+n) + \sin^2\left(\frac{\pi}{M}\right)}} \left[\frac{\pi}{2} + \tan^{-1}\left(\sqrt{\frac{\sin^2\left(\frac{\pi}{M}\right)}{\sigma^2(1+n)+\sin^2\left(\frac{\pi}{M}\right)}}\cot\left(\frac{\pi}{M}\right)\right)\right]. \tag{6}$$

Proof: The proof can be obtained by applying Binomial theorem and [19, eq.(5A.15)] to [18, eq.(30)] and [19, eq.(5.66)], and is omitted due to space limit. ■

Note that our Proposition 1 provides a simpler closed-form expression of $P_{s_{\text{singal}}}$ than [18, eq.(33)], which involved N_{g} number of infinite sums and still too complicated to compute.

Now, we focus on deriving the closed-form formulation for the second term of (3). To obtain the analytic expression of $\text{APEP}_{(k,m)\to(k',m')}$, it is indispensable to know the distribution of $|g_{(k)}s_m - g_{(k')}s_{m'}|$ when $k \neq k'$. This, in general, is a challenging task, but we are able to tackle this impediment. Let $\Psi \triangleq |g_{(k)}s_m - g_{(k')}s_{m'}|$ when $k \neq k'$. The complex random variable $g_{(k)}$ can be written as $g_{(k)} = r_k e^{j\theta_k}$, $k = 1,\ldots,K$ where $r_k = |g_{(k)}|$ and θ_k is the phase of $g_{(k)}$. For the $M-$PSK modulation, any symbol can be given as $s_m = e^{j\frac{2\pi m}{M}}, \forall m = 1,\ldots,M$. Then, we have $\Psi = \left|r_k e^{j\left(\theta_k + \frac{2\pi m}{M}\right)} - r_{k'}e^{j\left(\theta_{k'} + \frac{2\pi m'}{M}\right)}\right| = \left|r_k e^{j\left(\theta_k + \frac{2\pi m}{M}\right)} + r_{k'}e^{j\left(\theta_{k'} + \frac{2\pi m'}{M} + \pi\right)}\right|$. The PDFs of r_k and θ_k are given in the following Lemma 1.

Lemma 1: Given that $g_{(k)} = r_k e^{j\theta_k}$, $k = 1,\ldots,K$, $r_k = |g_{(k)}|, \forall k$ are iid. with pdf given as

$$f_{r_k}(x) = 2N_{\text{g}}xe^{-x^2}\left(1 - e^{-x^2}\right)^{N_{\text{g}}-1}. \tag{7}$$

The phase θ_k is uniformly distributed over the range $[0, 2\pi]$, i.e., $f_{\theta_k}(y) = \frac{1}{2\pi}$. And r_k and θ_k are independent .

Proof: See Appendix A. ■

From Lemma 1, we can see that r_k and $r_{k'}$ are iid., so do θ_k and $\theta_{k'}$; $\theta_k + \frac{2\pi m}{M}$ and $\theta_{k'} + \frac{2\pi m'}{M} + \pi$ are also uniformly distributed in $[0, 2\pi]$. This also implies that the $M-$PSK symbols have no impact on Ψ. By using the result of the distribution for the magnitude of the sum of complex random variables [21, Eq. (10)], the PDF of Ψ can be given as

$$f_{\Psi}(x) = xH_{0x}\{\Lambda(\rho)\} \tag{8}$$

where $H_{0x}\{\Lambda(\rho)\} = \int_0^{\infty} \rho J_0(x\rho)\Lambda(\rho)d\rho$ is the zero-order Hankel transform of function $\Lambda(\rho)$, $J_0(\cdot)$ is the zero-order Bessel function of the first kind, and $\Lambda(\rho) = \mathbb{E}_{r_k, r_{k'}}\left[J_0(r_k\rho)J_0(r'_k\rho)\right]$. Based on Lemma 1 and (8), we can acquire the following Lemma 2 and Proposition 2.

Lemma 2: The PDF of Ψ can be derived as

$$f_{\Psi}(x) = \sum_{n=0}^{N_{\mathrm{g}}-1} \sum_{l=0}^{N_{\mathrm{g}}-1} \frac{2(N_{\mathrm{g}}!)^2(-1)^{n+l} x e^{-\frac{(n+1)(l+1)}{n+l+2}x^2}}{n!(N_{\mathrm{g}}-1-n)!l!(N_{\mathrm{g}}-1-l)!(n+l+2)} \tag{9}$$

Proof: See Appendix B. ■

Proposition 2: The closed-form expression for $\mathrm{APEP}_{(k,m)\to(k',m')}$ can be derived as

$$\mathrm{APEP}_{(k,m)\to(k',m')} = \sum_{n=0}^{N_{\mathrm{g}}-1} \sum_{l=0}^{N_{\mathrm{g}}-1} \binom{N_{\mathrm{g}}}{n+1}\binom{N_{\mathrm{g}}}{l+1}\frac{(-1)^{n+l}}{2} \left[1 - \left(1 + \frac{4(n+1)(l+1)}{n+l+2}\sigma^2\right)^{-\frac{1}{2}}\right]. \tag{10}$$

Proof: See Appendix C. ■

Proposition 2 shows an interesting observation that given $k \neq k'$ and the $M-$PSK modulation, the $\mathrm{APEP}_{(k,m)\to(k',m')}$ in (10) is identical for any given set of $\{k, k', m, m'\}$. This is because i) all selected channels are iid; and ii) the effective phase distributions of channels after absorbing the impact of symbol are still iid uniform distributions. Thus for the presentation simplicity, we denote $\overline{\mathrm{APEP}} = \mathrm{APEP}_{(k,m)\to(k',m')}, \forall k \neq k', \forall m, m'$.Therefore, for the proposed OSM-MISO scheme, an explicit improved-union-bound can be derived as

$$P_{IU} = P_{s_{\mathrm{singal}}} + M(K-1)\overline{\mathrm{APEP}} \tag{11}$$

with closed-form expressions of $P_{s_{\mathrm{singal}}}$ and $\overline{\mathrm{APEP}}$ given in (6) of Proposition 1 and (10) of Proposition 2, respectively.

B. Comparisons between OSM and other TASS-SM scheme

We compare our OSM scheme with a popular low-complex TASS-SM schemes, i.e., COAS-SM, which chooses K out of N_{t} transmit antennas that corresponding to the first K largest channel gains [3]. Then, the conventional SM scheme is implemented on selected K antennas with $M-$ary APM symbols. Despite distinct antenna selections, the OSM and COAS-SM schemes support for the same data rate, i.e., $B = \log_2(KM)$ bpcu, and have identical set-up when $K = 1$ (pure antenna selection TAS) and $K = N_{\mathrm{t}}$ (conventional SM). However when $1 < K < N_{\mathrm{t}}$, with significantly dissimilar set-ups, our OSM outshines COAS-SM with following benefits.

Analytical tractability: The performance analysis of OSM scheme is tractable, as shown in Section III, benefit from its independent group antenna selection setting. On the contrary, although also being a low-complexity TASS-SM scheme, no much explicit analysis of the COAS-SM has been carried out [3]. And such analysis is challenging for COAS-SM, due to the coupling of order statistic distribution of selected K antennas, and the problem is greatly exacerbated by increasing the number of K. **Reduced feedback bits for CSI:** For both schemes, the receiver only needs to feedback the selected antenna indices to the transmitter. The COAS-SM scheme requires $\log_2^{\binom{N_{\mathrm{t}}}{K}}$ feedback bits, which is much larger than that of OSM scheme $K\log_2^{\frac{N_{\mathrm{t}}}{K}}$. E.g., when $N_t = 32$ and $K = 8$, the OSM and COAS-SM schemes will feedback at least 16 and 24 bits, respectively. **Lower complexity:** (1) For antenna selection - while the OSM scheme requires K times of sorting $\frac{N_{\mathrm{t}}}{K}$ elements, the COAS-SM requires sorting N_t elements which costs higher computations, e.g., when $N_t = 32$ and $K = 8$, the worst-case complexity ($\mathcal{O}\left(n^2\right)$) of the COAS-SM scheme is eight times higher than that of OSM scheme. (2) For analytical computation - Since there is no rigorous analytical expressions to calculate error rate of the COAS-SM scheme, we always need to perform Monte-Carlo simulations. Although the COAS-SM scheme may has low implement complexity, it consumes significant time for numerical evaluation, especially in high-SNR region.And the problem is dramatically aggravated by increasing the number of N_{t} and/or feedback bits B. Conversely, the high-SNR performance of the OSM scheme can be instantly computed by the derived explicit expressions with a high accuracy. **Superior performance at high SNR:** While the both scheme have similar performance at low SNR, the benefit of OSM scheme becomes more pronounced as SNR increases. Performance comparison is shown in Section IV.

IV. Numerical Result

In this section, we validate the derived theoretical expressions, and evaluate the performance of the proposed OSM-MISO scheme via numerical simulations. The performance is also compared with COAS-SM-MISO. It is important to note that, for a given number of transmit antennas N_{t}, in order to convey fixed B information bits, we may have different combinations of K (number of antenna groups) and M (modulation size), to achieve $\log_2 KM = B$ bits.

Fig. 3 shows the ASEP performance of OSM-MISO scheme versus the average SNR when $N_t = 8$ and $B = 6$ bits by considering some possible set of (K, M) combinations such as $(K, M) = \{(1, 64), (2, 32), (8, 8)\}$ ($(K, M) = (4, 16)$ case is omitted to make the figure less busy). It illustrates the accuracy of the improved union-bound (analytical expression (11)), by comparing with exact ASEP (Monte Carlo simulations) and the conventional union-bound. For all three cases, figure shows that the improved union-bound is more accurate than the union-bound as expected. Furthermore, improved union-bound is completely identical to the Monte Carlo results of $K = 1$ case (i.e., conventional TAS-MISO case) for the entire SNR region. It also well overlap with the exact performance of $K \geq 2$ cases for the moderate or high SNR region. These validate the explicit expressions of improved union-bound of OSM-MISO in (11), which thus can be employed to instantly and efficiently obtain the ASEP of OSM-MISO

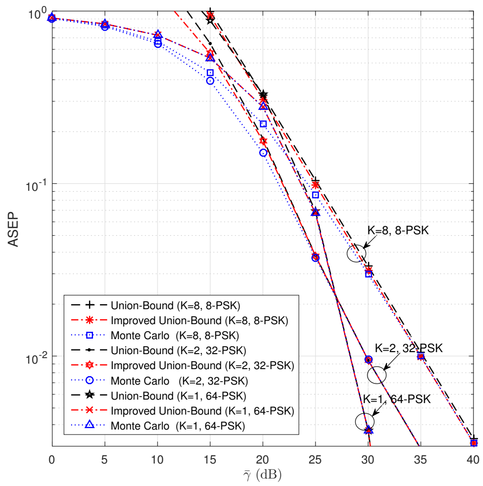

Fig. 3. Performance comparison among improved union-bound, exact ASEP and conventional union-bound, given $N_t = 8$ and 6 bits data rate

scheme at moderate-to-high SNR instead of Monte Carlo simulations. Fig.4 demonstrates the performance comparison between OSM-MISO and COAS-SM-MISO, for $N_t = 16$ with 4, 6, 8 bits data rate ($1 < K < N_t$) ($K = 4$ cases are omited to keep figure clear), respectively. From the Fig.4, we can see that for any given cases with $1 < K < N_t$, at low SNR, the performance of two schemes looks very similar, however, as SNR increases, OSM-MISO clearly exhibits pronounced advantage and outshines COAS-SM-MISO, especially for small K cases. Although, at high SNR, both schemes fail to offer the transmit diversity, the coding gain of our OSM scheme surpasses that of the COAS-SM scheme. This confirm that OSM-MISO is a more effective low-complexity TASS-SM scheme than the existing COAS-SM-MISO.

V. Conclusions and Possible Extensions to OSM-MIMO Systems

In this paper, a novel and tractable low-complexity TASS-SM scheme, OSM, is proposed to enhance system reliability. We develop a closed-form expression for error performance of OSM-MISO system over Rayleigh fading channels. By comparing to a prevalent TASS-SM scheme (COAS-SM), OSM shows excellent and appealing performance-complexity trade-off. The concept and the results of OSM-MISO can be easily extended to MIMO systems, i.e.,more than one receive antenna, with a priori best single-antenna selection on the receiver side as well.

Appendix

A. Proof of Lemma 1

Let $h_i = b_i e^{j\phi_i}, \forall i = 1, \ldots N_t$, where $b_i = |h_i|$ is the magnitude of h_i and ϕ_i is the phase. Since $h_i \sim \mathcal{CN}(0,1)$, b_i follows the Rayleigh distribution as $f_{b_i}(u) = 2ue^{-u^2}$, and b_i^2 follows the exponential distribution as $f_{b_i^2}(v) = e^{-v}$. The phase ϕ_i is uniformly distributed over the range $[0, 2\pi]$, i.e., $f_{\phi_i}(t) = \frac{1}{2\pi}$, and it is independent of b_i. For Group $k, \forall k = 1, \ldots, K$, as $N_{(k)} = \arg \max_{k(N_g-1)+1 \le i \le kN_g} b_i^2$, the joint CDF of the magnitude and phase of $g_{(k)}$ is given as

$$
\begin{aligned}
&F_{(r_k,\theta_k)}(x, y) \\
&= \Pr\left\{ b_{N_{(k)}} \le x, \phi_{N_{(k)}} \le y \middle| b_{N_{(k)}}^2 = \max_{k(N_g-1)+1 \le i \le kN_g} b_i^2 \right\} \\
&= \frac{\Pr\left\{ b_{N_{(k)}} \le x, \phi_{N_{(k)}} \le y, b_{N_{(k)}}^2 = \max_{k(N_g-1)+1 \le i \le kN_g} b_i^2 \right\}}{\Pr\left\{ b_{N_{(k)}}^2 = \max_{i=k(N_g-1)+1}^{kN_g} b_i^2 \right\}} \\
&= \frac{\left(\int_0^y \frac{dt}{2\pi}\right) \int_0^x \left(\int_0^{u^2} e^{-v} dv\right)^{N_g-1} 2ue^{-u^2} du}{\int_0^\infty \left(\int_0^{u^2} e^{-v} dv\right)^{N_g-1} 2ue^{-u^2} du} \\
&= \frac{y}{2\pi} \left(1 - e^{-x^2}\right)^{N_g}. \qquad (12)
\end{aligned}
$$

Thus, the CDF of r_k is given as $F_{r_k}(x) = F_{(r_k,\theta_k)}(x, 2\pi) = \left(1 - e^{-x^2}\right)^{N_g}$ and the CDF of θ_k is given as $F_{\theta_k}(y) = F_{(r_k,\theta_k)}(\infty, y) = \frac{y}{2\pi}$. Since we have $F_{(r_k,\theta_k)}(x, y) = F_{r_k}(x) F_{\theta_k}(y)$, random variables r_k and θ_k are independent. The PDFs of r_k and θ_k can be obtained respectively as $f_{r_k}(x) = \frac{\partial F_{r_k}(x)}{\partial x} = 2N_g \left(1 - e^{-x^2}\right)^{N_g-1} xe^{-x^2}$, and $f_{\theta_k}(y) = \frac{\partial F_{\theta_k}(y)}{\partial y} = \frac{1}{2\pi}$.

B. Proof of Lemma 2

r_k and $r_{k'}$ are i.i.d. with the pdf given in Lemma 1, then,

$$
\begin{aligned}
&\Lambda(\rho) = \left(\mathbb{E}_{r_k}\left[J_0(r_k\rho)\right]\right)^2 \\
&= \left(\int_0^\infty J_0(r_k\rho) 2N_g \left(1 - e^{-r_k^2}\right)^{N_g-1} r_k e^{-r_k^2} dr_k\right)^2 \\
&\overset{\text{let } t \triangleq r_k^2}{=} \left(N_g \int_0^\infty J_0(\sqrt{t}\rho)\left(1 - e^{-t}\right)^{N_g-1} e^{-t} dt\right)^2 \\
&\overset{(a)}{=} \left(\sum_{n=0}^{N_g-1} \frac{N_g!(-1)^n}{n!(N_g-1-n)!} \int_0^\infty J_0(\sqrt{t}\rho) e^{-(n+1)t} dt\right)^2 \\
&\overset{(b)}{=} \left(\sum_{n=0}^{N_g-1} \frac{N_g!(-1)^n}{(n+1)!(N_g-1-n)!} e^{-\frac{\rho^2}{4(n+1)}}\right)^2 \\
&= \sum_{n=0}^{N_g-1} \sum_{l=0}^{N_g-1} \frac{(N_g!)^2(-1)^{n+l} e^{-\frac{n+l+2}{4(n+1)(l+1)}\rho^2}}{(n+1)!(N_g-1-n)!(l+1)!(N_g-1-l)!}
\end{aligned}
\qquad (13)
$$

where (a) is obtained by applying the Binomial theorem $(1 + x)^n = \sum_{i=0}^n \frac{n!}{i!(n-i)!} x^i$ and (b) is due to $\int_0^\infty J_0(b\sqrt{x}) e^{-ax} dx = \frac{1}{a} e^{-\frac{b^2}{4a}}$ [22, eq 6.614] . Substituting (13) into (8), we have,

$$
\begin{aligned}
&f_\Psi(x) = x \int_0^\infty \rho J_0(x\rho) \Lambda(\rho) d\rho \\
&= \sum_{n=0}^{N_g-1} \sum_{l=0}^{N_g-1} \frac{(N_g!)^2(-1)^{n+l} x \int_0^\infty \rho J_0(x\rho) e^{-\frac{n+l+2}{4(n+1)(l+1)}\rho^2} d\rho}{(n+1)!(N_g-1-n)!(l+1)!(N_g-1-l)!} \\
&\overset{(c)}{=} \sum_{n=0}^{N_g-1} \sum_{l=0}^{N_g-1} \frac{2(N_g!)^2(-1)^{n+l} x e^{-\frac{(n+1)(l+1)}{n+l+2}x^2}}{n!(N_g-1-n)! l!(N_g-1-l)!(n+l+2)}
\end{aligned}
\qquad (14)
$$

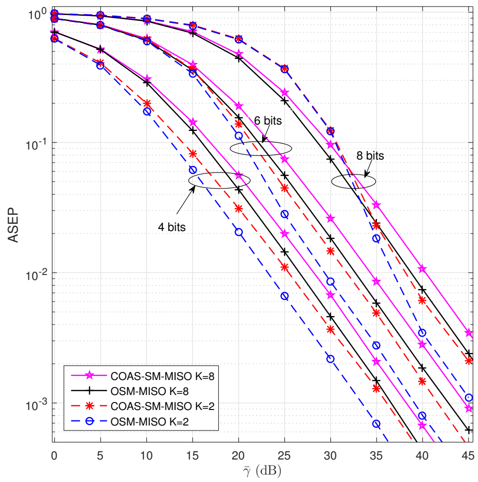

Fig. 4. Comparison between OSM-MISO and COAS-SM-MISO for $N_t = 16$ with $4, 6, 8$ bits data rate, respectively.

where (c) is due to changing variable ρ to ρ^2 and then applying [22, eq 6.614].

C. Proof of Proposition 2

From (4), we have,

$$
\begin{aligned}
&\mathrm{APEP}_{(k,m)\to(k',m')} = \mathbb{E}_{\mathbf{g}}\left[Q\left(\sqrt{\frac{|g_{(k)}s_m - g_{(k')}s_{m'}|^2}{2\sigma^2}}\right)\right] \\
&= \int_0^\infty Q\left(\frac{x}{\sqrt{2}\sigma}\right) f_\Psi(x)dx \\
&\overset{(a)}{=} \int_0^\infty Q\left(\frac{x}{\sqrt{2}\sigma}\right) x \int_0^\infty \rho J_0(x\rho)\Lambda(\rho)d\rho dx \\
&\overset{(b)}{=} \frac{1}{2}\int_0^\infty e^{-\beta}[I_0(\beta) - I_1(\beta)]\Lambda\left(\frac{\sqrt{2\beta}}{\sigma}\right)d\beta \qquad (15)
\end{aligned}
$$

(a) is due to applying the integral representation of $f_\Psi(x)$ from (8) and (b) is obtained by applying [23, eq.(20)]. Substituting (13) into (15), we have,

$$
\begin{aligned}
&\mathrm{APEP}_{(k,m)\to(k',m')} = \\
&\frac{1}{2}\sum_{n=0}^{N_g-1}\sum_{l=0}^{N_g-1} \frac{(N_g!)^2(-1)^{n+l}}{(n+1)!(N_g-1-n)!(l+1)!(N_g-1-l)!} \\
&\int_0^\infty [I_0(\beta) - I_1(\beta)]e^{-\beta\left(\frac{n+l+2}{2\sigma^2(n+1)(l+1)}+1\right)}d\beta \qquad (16)
\end{aligned}
$$

According to [22, eq 6.611.4], we can get $\int_0^\infty I_0(\beta)e^{-c\beta}d\beta = \frac{1}{\sqrt{c^2-1}}$, $c > 1$ and $\int_0^\infty I_1(\beta)e^{-c\beta}\, d\beta = \frac{c}{\sqrt{c^2-1}} - 1$. Thus we have,

$$
\int_0^\infty [I_0(\beta) - I_1(\beta)]e^{-c\beta}d\beta = 1 - \sqrt{\frac{c-1}{c+1}}, \quad c > 1. \qquad (17)
$$

Applying (17) into (16), the closed-form expression of $\mathrm{APEP}_{(k,m)\to(k',m')}$ in (10) is obtained.

References

[1] M. D. Renzo, H. Haas, A. Ghrayeb, S. Sugiura, and L. Hanzo, "Spatial modulation for generalized MIMO: Challenges, opportunities, and implementation," *Proc. IEEE*, vol. 102, no. 1, p. 56103, Jan. 2014.

[2] M. D. Renzo and H. Haas, "On transmit diversity for spatial modulation MIMO: Impact of spatial constellation diagram and shaping filters at the transmitter," *IEEE Trans. Veh. Technol.*, vol. 62, no. 6, pp. 2507–2531, Jul. 2013.

[3] R. Rajashekar, K. V. S. Hari, and L. Hanzo, "Antenna selection in spatial modulation systems," *IEEE Commun. Lett.*, vol. 17, no. 3, pp. 521 – 524, Mar. 2013.

[4] Z. Zhou, N. Ge, and X. Lin, "Reduced-complexity antenna selection schemes in spatial modulation," *IEEE Commun. Lett.*, vol. 18, no. 1, pp. 14 – 17, Jan. 2014.

[5] P. Yang, Y. Xiao, L. Li, Q. Tang, Y. Yu, and S. Li, "Link adaptation for spatial modulation with limited feedback," *IEEE Trans. Veh. Technol.*, vol. 61, no. 8, pp. 3808–3813, Oct. 2012.

[6] R. Rajashekar, K. V. S. Hari, and L. Hanzo, "Quantifying the transmit diversity order of euclidean distance based antenna selection in spatial modulation," *IEEE Signal Processing Lett.*, vol. 22, no. 9, pp. 1434 – 1437, Sep. 2015.

[7] N. Pillay and H. Xu, "Comments on antenna selection in spatial modulation systems," *IEEE Commun. Lett.*, vol. 17, no. 9, pp. 1681 – 1683, Sep. 2013.

[8] K. Ntontin, M. D. Renzo, A. I. Prez-Neira, and C. Verikoukis, "A low-complexity method for antenna selection in spatial modulation systems," *IEEE Commun. Lett.*, vol. 17, no. 12, pp. 2312 – 2315, Dec. 2013.

[9] M. Maleki, H. R. Bahrami, and A. Alizadeh, "Adaptive antenna subset selection and constellation breakdown for spatial modulation," *IEEE Commun. Lett.*, vol. 18, no. 9, pp. 1649 – 1652, Sep. 2014.

[10] N. Wang, W. Liu, H. Men, M. Jin, and H. Xu, "Further complexity reduction using rotational symmetry for edas in spatial modulation," *IEEE Commun. Lett.*, vol. 18, no. 10, pp. 1835 –1838, Oct. 2014.

[11] J. Zheng and J. Chen, "Further complexity reduction for antenna selection in spatial modulation systems," *IEEE Commun. Lett.*, vol. 19, no. 6, pp. 937 –940, Jun. 2015.

[12] Z. Sun, Y. Xiao, L. You, L. Yin, P. Yang, and S. Li, "Cross-entropy-based antenna selection for spatial modulation," *IEEE Commun. Lett.*, vol. 20, no. 3, pp. 622 –625, Mar. 2016.

[13] P. Yang, Y. Xiao, Y. L. Guan, S. Li, and L. Hanzo, "Transmit antenna selection for multiple-input multiple-output spatial modulation systems," *IEEE Trans. Commun.*, vol. 64, no. 5, pp. 2035–2048, May 2016.

[14] Z. Sun, Y. Xiao, P. Yang, S. Li, and W. Xiang, "Transmit antenna selection schemes for spatial modulation systems: Search complexity reduction and large-scale mimo applications," *IEEE Trans. Veh. Technol.*, vol. 66, no. 9, pp. 8010–8021, 2017.

[15] R. Rajashekar, K. Hari, and L. Hanzo, "Transmit antenna subset selection in spatial modulation relying on a realistic error-infested feedback channel," *IEEE Access*, no. 99, Oct. 2017.

[16] ——, "Transmit antenna subset selection for single and multiuser spatial modulation systems operating in frequency selective channels," *Submitted to IEEE Transactions on Vehicular Technology*, Oct. 2017.

[17] M. D. Renzo and H. Haas, "Bit error probability of SM-MIMO over generalized fading channels," *IEEE Trans. Veh. Technol.*, vol. 61, no. 3, pp. 1124 – 1144, Mar. 2012.

[18] Z. Chen, Z. Chi, Y. Li, and B. Vucetic, "Error performance of maximal-ratio combining with transmit antenna selection in flat Nakagami-m fading channels," *IEEE Trans. Wireless Commun.*, vol. 8, no. 1, pp. 424 – 431, Jan. 2009.

[19] M. K. Simon and M.-S. Alouini, *Digital Communication over Fading Channels: A Unified Approach to Performance Analysis*. New York: John Wiley & Sons, 2000.

[20] H. A. David and H. N. Nagaraja, *Order Statistics*, 3rd ed. Wiley Series in Probability and Statistics, 2005.

[21] A. Abdi, H. Hashemi, and S. Nader-Esfahani, "On the pdf of the sum of random vectors," *IEEE Trans. Commun.*, vol. 48, no. 1, pp. 7 – 12, Jan. 2000.

[22] D. Zwillinger, *Table of Integrals, Series, and Products*, 8th ed. Elsevier Science, 2014.

[23] Z. Du, J. Cheng, and N. C. Beaulieu, "Accurate error-rate performance analysis of OFDM on frequency-selective Nakagami-m fading channels," *IEEE Trans. Commun.*, vol. 54, no. 2, pp. 319 – 328, Feb. 2006.